ELSEVIER

Catalysis Today 58 (2000) 233–240

CATALYSIS TODAY

www.elsevier.com/locate/cattod

The synthesis of attrition resistant slurry phase iron Fischer–Tropsch catalysts

Hien N. Pham, Abhaya K. Datye*

Center for Microengineered Materials, Department of Chemical and Nuclear Engineering, University of New Mexico, Albuquerque, NM 87131-1341, USA

Abstract

We describe the evolution of catalyst microstructure as a precipitated Fe–Cu catalyst precursor is transformed into an attrition resistant Fischer–Tropsch (F–T) catalyst. The precipitated Fe–Cu catalyst, as-prepared, is weak compared to the same catalyst that was spray-dried, but without a binder. Spray-drying improves the attrition resistance of the catalyst. Ultrasonic fragmentation was used in this work to measure the attrition resistance of the slurry phase catalysts. Both catalysts, after ultrasonication, produce fine particles below 5 μm, which could cause filtration problems in slurry F–T reactors. The addition of silica as the binder improved the catalyst's attrition resistance with negligible generation of fine particles below 5 μm. Cross-section TEM of the SiO_2-containing Fe F–T catalyst shows that the crystallized Fe particles with an average particle diameter of 80 nm are uniformly distributed within a silica binder. This study provides insight into the catalyst microstructure that leads to improved attrition resistance in Fe F–T catalysts.

Keywords: Fischer–Tropsch catalyst; Fe–Cu catalyst; Attrition

1. Introduction

This work is directed towards synthesis of attrition resistant Fe Fischer–Tropsch (F–T) catalysts. In a previous study [1], we reported a comparison of two approaches used for measuring the attrition strength of catalyst agglomerates: ultrasonic fragmentation and uniaxial compaction. Ultrasonic fragmentation coupled with particle size distribution measurements was found to be more sensitive to differences in catalyst strength than uniaxial compaction. Recently, we have also explored the role of binder morphology to provide improved attrition resistance to the Fe F–T catalysts. Using the ultrasonic fragmentation approach [2,3] we concluded that a plate-like kaolin binder did not impart any additional strength to a precipitated Fe catalyst. As revealed by TEM [1], the kaolin and Fe F–T catalyst occurred as two distinct phases, and both had plate-like structures which did not connect to create strong interlocking forces between them. Hence, a precipitated silica was chosen as the binder. The silica provides a morphology that is conducive to creating interlocking forces that hold the Fe F–T catalyst together.

There are several processing steps such as calcination and silica binder addition (either before or after spray-drying) that affect the attrition resistance of the catalyst [4]. We concluded that the addition of precipitated silica to the Fe–Cu precursor followed by spray-drying produces a catalyst with superior attrition resistance. Not only is the spray-dried Fe F–T catalyst attrition resistant, its spherical shape may provide

* Corresponding author. Tel.: +1-505-277-0477; fax: +1-505-277-1024.
E-mail address: datye@unm.edu (A.K. Datye)

0920-5861/00/$ – see front matter
PII: S0920-5861(00)00256-X

better hydrodynamics when the catalyst is used in a slurry bubble-column reactor.

In this study, we examine the evolution of catalyst morphology during the synthesis of Fe F–T catalysts. The attrition strength of the catalyst was related to its microstructure during the various steps in the synthesis of this Fe F–T catalyst: the as-prepared precipitated Fe–Cu precursor, after spray-drying, and the addition of precipitated silica followed by spray-drying. Techniques such as ultrasonic fragmentation, transmission electron microscopy (TEM) and scanning electron microscopy (SEM) were used for the analysis. Some of the catalyst samples were studied using cross-section, which was recently applied to the study of Fe F–T catalysts [5].

2. Experimental

A precipitated Fe–Cu catalyst (64.80% Fe, 6.24% Cu by ICP based on dried weight) in its wet form (labeled PRFECU-ED20-124) was used for the experiments. The starting materials were the nitrates of Fe and Cu, and NH_4OH. Solutions of Fe–Cu nitrate and NH_4OH were mixed at 80°C in a continuous flow through mixer, causing the iron oxide to precipitate. The product catalyst was discarded until the pH was between 6.8 and 7.2. The catalyst was then collected in a filter funnel, and the filter cake was pumped down to being wet but not cracked. Samples of the filtrate were obtained; a pH and brown-ring test were performed for each sample to ensure that the pH remained near 7.0 and that traces of NH_4NO_3 were removed from the catalyst, respectively. The cake was removed and then re-suspended in hot water. After filtering the slurry, samples of the filtrate were obtained for pH and brown-ring testing. After the brown-ring test was negative, the filter cake was pumped moist. Finally, once the precipitated Fe–Cu catalyst was dry enough to remove it off the filter, the catalyst was suspended in deionized H_2O.

One hundred milliliters of the precipitated Fe–Cu catalyst was ultrasonicated at an amplitude of 20 for 2 min to break up any loose agglomerates. A Tekmar 501 ultrasonic disrupter (20 kHz±50 Hz) equipped with a V1A horn and a $\frac{1}{2}$ in probe tip was used for the ultrasonication process. The sample was then mixed with 11 ml of potassium silicate solution (KASIL® #1; PQ Corp.), to yield a silica loading of 25 wt.%. Diluted nitric or hydrochloric acid (0.1 N; J.T. Baker) was added dropwise while the slurry was stirred until the pH was about 7. Deionized water was added to prepare 250 ml of slurry, and the mixture was stirred for ≈10 min. A Buchi 190 Mini Spray Dryer was used to spray-dry the slurry. The inlet temperature of the spray dryer was over 200°C with the outlet being maintained over 100°C.

A Micromeritics Sedigraph 5100 analyzer was used to measure the particle size distribution with time. One gram of the catalyst sample was added to 50 ml of a 0.05 wt.% solution of sodium hexametaphosphate (SHMP), which was used to prevent flocculation during the size determination. The suspension was then subjected to ultrasound at 5-min intervals using the Tekmar 501 ultrasonic disrupter, at an amplitude setting of 20. After different extents of ultrasonic irradiation, the particle size distribution was analyzed to detect the extent of particle fragmentation. The size distribution also revealed whether particle fracture occurred (with a shift in median size) or erosion (showing the appearance of fine particles).

The precipitated iron catalyst precursor as well as the spray-dried catalyst was examined using electron microscopy. SEM was performed using a Hitachi S-800 field emission gun SEM while a 200 kV JEOL 2010 TEM was used for higher magnification images. The spray-dried catalyst was examined by cross-section TEM. The details of sample preparation and the conditions used for microtomy are described elsewhere [5]. Cross-sections having a thickness of 60 nm were prepared and holey carbon grids (SPI Supplies) were used to pick up the thin sections for TEM analysis.

3. Results and discussion

Fig. 1 shows cumulative mass distribution plots of mass finer (%) vs. equivalent spherical diameter for the precipitated Fe–Cu catalyst, both as-prepared and after spray-drying. The as-prepared catalyst breaks down easily after 25 min of ultrasonic irradiation, and has a broad particle size distribution. On the other hand, spray-drying improves the attrition resistance of the precipitated Fe–Cu catalyst, which has a more uniform particle size distribution. There is some

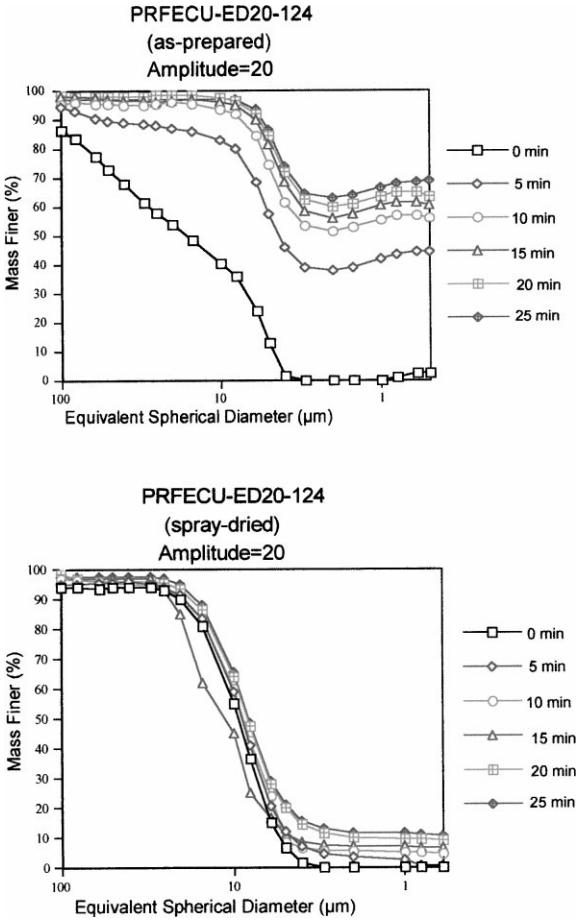

Fig. 1. Sedigraph particle size distributions of a precipitated Fe–Cu catalyst, as-prepared and after spray-drying. The as-prepared catalyst is weak and breaks down easily after 25 min of ultrasonic irradiation, while spray-drying improves its attrition resistance.

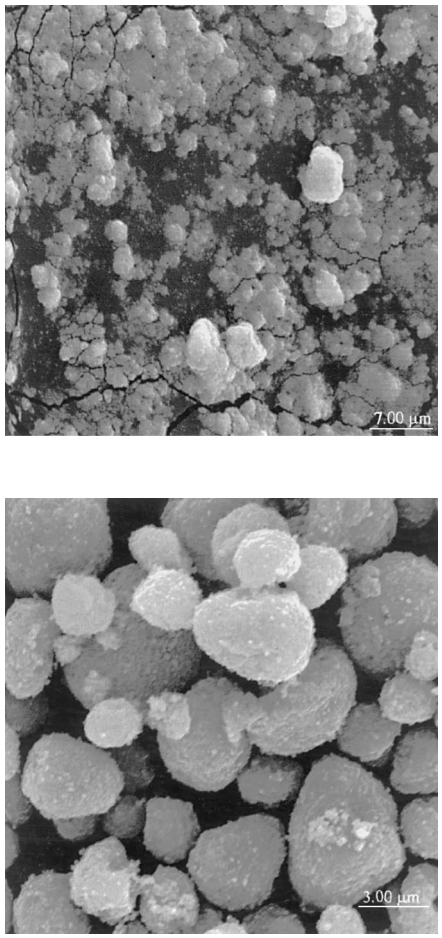

Fig. 2. SEM images of the precipitated Fe–Cu catalyst precursor, as-prepared and after spray-drying. The as-prepared catalyst particles are clustered together due to drying of the catalyst, which is initially present in a suspension. The spray-dried catalyst below consists of individual agglomerates.

generation of fine particles below 5 μm, suggesting that the catalyst is still not resistant to erosion. The generation of fine particles below 5 μm due to erosion may not, however, be acceptable for slurry F–T reactors. Fig. 2 shows SEM images of these catalysts. The spray-dried catalyst consists of individual agglomerates compared to the catalyst, as-prepared. Since the as-prepared catalyst is initially in its wet form, drying the catalyst causes the particles to cluster together. Therefore, the micron-sized particles seen in this image are actually composed of individual primary particles, as we show below. In addition, there appears to be a thin film in the SEM image in addition to these agglomerates. The resolution of the SEM is not sufficient to determine the nature of the individual particles that make up this film. Therefore, a TEM was used to study the primary particles in this precipitated iron catalyst.

The precipitated Fe–Cu precursor in its wet form was first allowed to settle overnight. A drop of the supernatant suspension was then deposited on a TEM grid to better characterize the morphology of the iron phase in this catalyst precursor. Fig. 3A shows a TEM image of the precipitated Fe–Cu precursor from the supernatant solution. This image shows that the

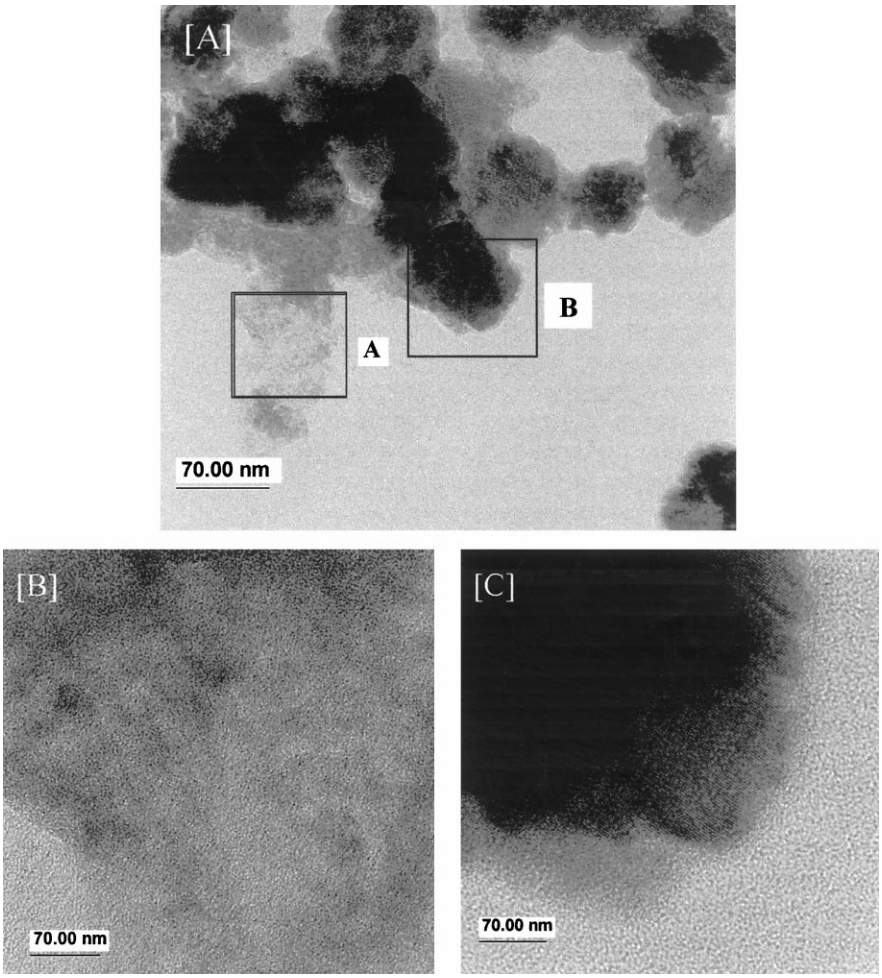

Fig. 3. (A) TEM image of the precipitated Fe–Cu catalyst precursor from the supernatant solution. (B) An amorphous phase, region A, which indicates it is too thin to have fully crystallized. (C) Lattice fringes, region B, confirm that the primary particles are all single crystals.

supernatant contains primary particles which can be indexed based on X-ray diffraction to be crystalline hematite (Fe_2O_3). A higher magnification view of one of these particles is shown in Fig. 3C. The lattice fringes confirm that the primary particles are all single crystals even though they have very irregular outlines and show no well-defined facets. The area labeled A in Fig. 3A is also shown at a higher magnification in Fig. 3B. It is evident that this region is amorphous, which could indicate it is too thin to have fully crystallized. It is clear that the supernatant suspension contains only crystalline primary particles.

To examine the rest of the precursor solution, it was re-suspended using ultrasonication to break up any loose agglomerates. A drop of this suspension was deposited on a TEM grid for examination to see if the nature of the primary particles was any different from that in the supernatant. Fig. 4 shows a TEM image of the precipitated Fe–Cu precursor from the ultrasonicated solution. Roughly spherical particles are seen that are very similar to those seen in Fig. 3A, with an average primary particle size of 80 nm. Higher magnification views show no evidence of any amorphous thin film to be present on the carbon support film. Therefore, we conclude that the wet catalyst

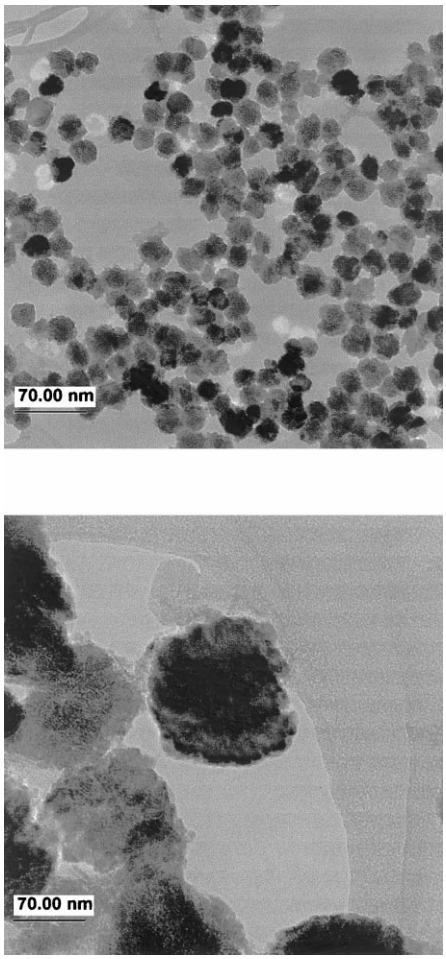

Fig. 4. TEM image of the precipitated Fe–Cu catalyst precursor, obtained from the ultrasonicated solution. The catalyst consists of crystalline primary particles of hematite with an average particle size of 80 nm. A higher magnification view is shown below.

precursor contains only crystalline primary particles, and there is no evidence for any soluble iron species still left in solution.

The next step in the synthesis was the addition of silica to these hematite particles. We investigated various approaches to adding the SiO_2 to the precursor, both before and after spray-drying, and also explored the role of a calcination step [4]. It was found that the addition of the SiO_2 binder before spray-drying was most beneficial, subsequent calcination providing no further improvement in strength. Catalysts that were calcined first, before spray-drying, were even stronger,

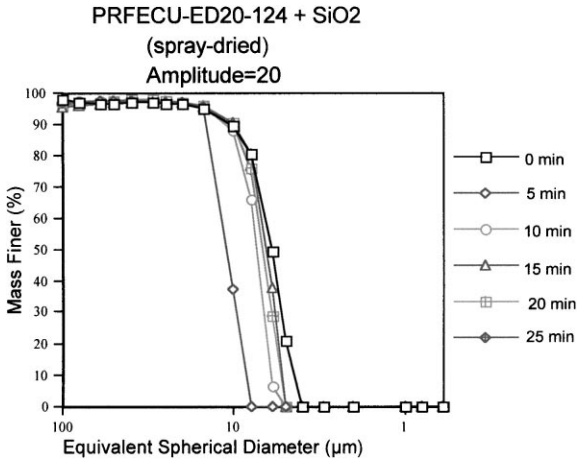

Fig. 5. Sedigraph particle size distribution of a spray-dried precipitated Fe–Cu catalyst containing silica. There is little generation of fine particles below 5 μm after 25 min of ultrasonic irradiation.

but the aggregates were irregularly shaped [4]. Hence, in this study, we restricted ourselves to spray-dried catalysts where silica was added before the spray-drying step.

Fig. 5 shows the particle size distribution of the SiO_2-containing catalyst, before and after ultrasonic irradiation. It is clear that the presence of silica further improves the attrition resistance of the catalyst. There is no generation of fine particles below 5 μm even after 25 min of ultrasonic irradiation. BET surface area, pore volume and bulk density of the spray-dried catalyst are 127.5 m^2/g, 0.18 cm^3/g and 1.67 g/cm^3, respectively. Fig. 6 shows an SEM image of the SiO_2-containing spray-dried Fe–Cu catalyst. The catalyst is roughly spherical in shape, typical of a spray-drying process, but the median particle size (≈8 μm) is smaller than that desired for a commercial F–T process (50–70 μm). This represents a limitation of our bench-top spray dryer. The SEM image does not provide any clues to the particle–binder interaction. For example, we cannot determine the morphology of the SiO_2 binder and the distribution of the hematite particles within the agglomerate. Hence, cross-section transmission electron microscopy (XTEM) was performed to look more closely at particle–binder interactions, and to map out the internal structure of the catalyst agglomerates. The particle outlined by the circle in Fig. 6 shows a typical catalyst agglomerate that was analyzed by XTEM.

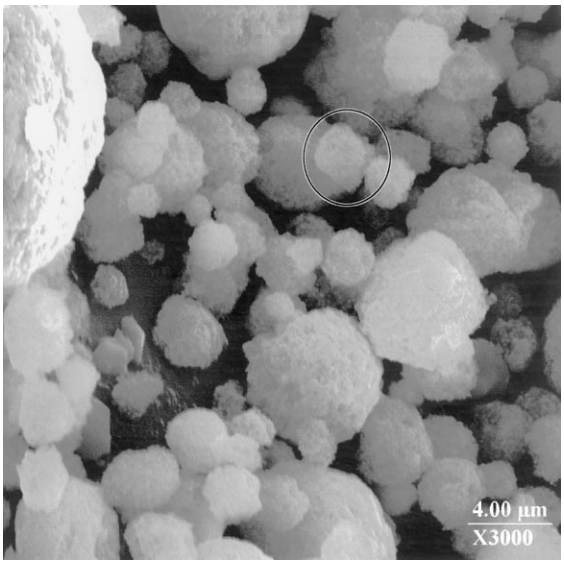

Fig. 6. SEM image of the spray-dried precipitated Fe–Cu catalyst containing SiO_2. A typical catalyst agglomerate analyzed by cross-section TEM in Fig. 7 is outlined by the circle.

XTEM images of the SiO_2-containing spray-dried Fe–Cu catalyst are shown in Fig. 7. Some of the catalyst agglomerates were broken apart due to the force exerted by the diamond knife during the microtoming process. The XTEM image in Fig. 7B is an example of an unbroken catalyst agglomerate. The dark-colored areas in the catalyst agglomerate represent the crystalline hematite particles surrounded by the amorphous SiO_2 binder. The particle size appears similar to that seen by TEM before addition of silica, with an average particle size of about 88 nm. The overall size of the catalyst agglomerate (Fig. 7A) is in agreement with the agglomerate sizes seen in the SEM image (Fig. 6).

Fig. 8 shows an XTEM image of the catalyst at a higher magnification. Region A comprised 70 wt.% of Fe and 5 wt.% of Si. Region B shows a significant amount of hematite to be present even though the TEM image shows contrasting characteristics of amorphous silica (23 wt.% Fe vs. 33 wt.% Si). The presence of an iron phase in areas of the sample that are devoid of the crystalline particles is surprising. The initial analysis of the precursor had ruled out any soluble species being present in the precursor. Therefore, we feel that a possible explanation is that some of the particles in the precursor, particularly the thin amorphous regions

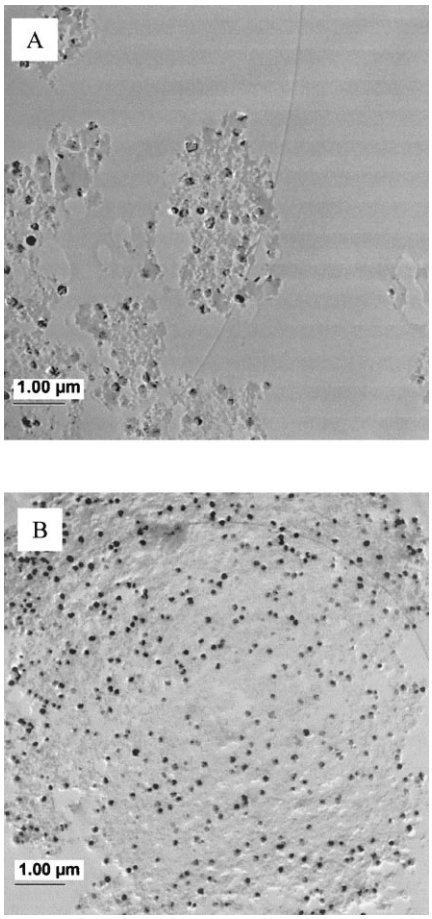

Fig. 7. XTEM image of the spray-dried precipitated Fe–Cu–SiO_2 catalyst. (A) Aggregates that may have broken up due to the forces exerted during microtoming. The dark spots are hematite particles in a silica matrix. (B) An unbroken catalyst agglomerate.

such as shown in Fig. 3B, may dissolve during the acid addition to cause silica precipitation from the silicate solution. The iron present on the silica is in highly dispersed form and does show up as a crystalline phase that can be identified in TEM images.

The compositions of Fe and Si obtained by EDS analysis via TEM were compared with the compositions obtained by X-ray photoelectron spectroscopy (XPS). Table 1 gives wt.% compositions for the Fe, Si and O elements. The wt.% of Fe from XPS is less than the wt.% of Fe determined from EDS analysis (22 vs. 37%, respectively). XPS sees only the near-surface region of the sample, whereas EDS is bulk analysis.

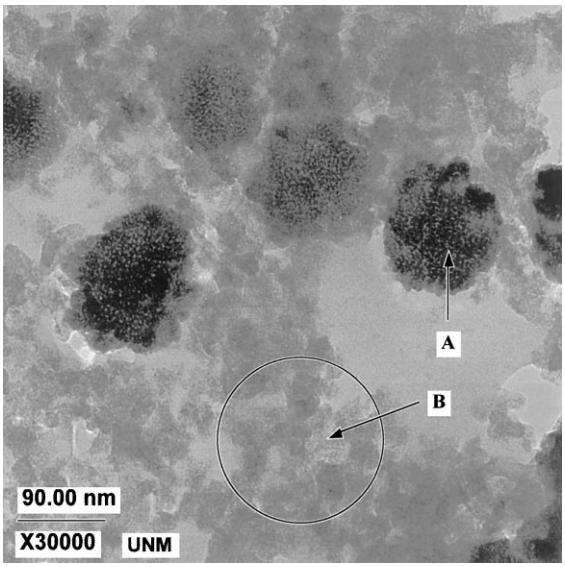

Fig. 8. XTEM image of the spray-dried precipitated Fe–Cu catalyst containing a SiO_2 binder. Region A mostly consists of iron oxide while region B consists of amorphous silica with some iron phase present.

Table 1
Elemental analysis of the Fe–Cu–SiO_2 spray-dried catalyst

Elements	From EDS (wt.%)	From XPS (wt.%)
Fe	37.23	21.68
Si	23.88	22.36
O	38.05[a]	50.99[a]

[a]Based on calculations of iron oxide and silica.

Based on these differing analyses, we can conclude that the surface of the catalyst must be richer in silica than the bulk. The cross-section TEM indeed shows very few of the hematite particles near the perimeter of the catalyst agglomerate.

4. Summary

We have examined the various steps in the synthesis of Fe F–T catalysts and correlated the microstructure with the attrition resistance of the agglomerates. The precipitated Fe–Cu catalyst consists of crystalline particles with an average primary particle size of 80 nm. In its as-prepared state, the precipitated Fe–Cu catalyst is weak and breaks down easily after applying ultrasound. Spray-drying this catalyst precursor improves the attrition resistance of the catalyst. However, there is still some generation of fine particles below 5 μm due to erosion, suggesting that a binder may be essential for providing attrition resistance to the Fe F–T catalyst.

Addition of precipitated silica, followed by spray-drying, further improved the attrition resistance of the Fe F–T catalyst, showing no generation of fine particles below 5 μm after 25 min of ultrasonic irradiation. The median particle size of these spray-dried agglomerates was about 8 μm, which was the best we could achieve with our bench-top spray dryer. These agglomerates contain crystalline particles of hematite dispersed uniformly within an amorphous silica matrix.

In future work, these spray-dried catalysts will be tested under actual F–T conditions, and then analyzed to determine their particle size distributions. It is known that iron oxide catalysts first have to be transformed into reduced iron phases, such as iron carbides, before they achieve a high activity for F–T synthesis reactions [6]. However, these phase transformations result in a chemical attrition of the catalyst [7], which needs to be considered in the design of attrition-resistant catalysts.

Acknowledgements

We thank the US Department of Energy, Federal Energy Technology Center (FETC), University Coal Research (UCR) program, for support of this research under contract numbers DE-FG22-95PC95210 and DE-FG26-98FT40110. We thank Yaming Jin for help with the cross-section TEM and Robert Gormley at FETC for providing us with the catalyst precursor, and for helpful discussions.

References

[1] H.N. Pham, J. Reardon, A.K. Datye, Powder Technol. 103 (1999) 95.
[2] S.G. Thoma, M. Ciftcioglu, D.M. Smith, Powder Technol. 68 (1991) 53.
[3] S.G. Thoma, M. Ciftcioglu, D.M. Smith, Powder Technol. 68 (1991) 71.

[4] H.N. Pham, A. Viergutz, R.J. Gormley, A.K. Datye, Powder Technol., 2000 (in press).
[5] Y. Jin, Phase transformations of iron-based catalysts for Fischer–Tropsch synthesis, Dissertation, University of New Mexico, Spring, 1999.
[6] M.D. Shroff, D.S. Kalakkad, K.E. Coulter, S.D. Kohler, M.S. Harrington, N.B. Jackson, A.G. Sault, A.K. Datye, J. Catal. 156 (1995) 185.
[7] D.S. Kalakkad, M.D. Shroff, S. Kohler, N. Jackson, A.K. Datye, Appl. Catal. 133 (1995) 335.